Nuclear structure for the isotopes ^{3}He and ^{4}He in k$^+$N scattering

R. Arceo
Centro de Investigación y Desarrollo del Estado de Michoacán.
Morelia, Michoacán 58060, México.
Escuela Superior de Física y Matemáticas, Instituto Politécnico Nacional,
Edificio 9, 07738 México D.F., México.
e-mail: rarceo@nmsu.edu.

Recibido el 15 de octubre de 2007; aceptado el 3 de abril de 2008

The study of the nuclear structure of ^{3}He and ^{4}He was performed by using K$^+$N phase shifts at incident energies up to 900 MeV. The analysis and comparison with previous experiments and theoretical results were made, obtaining better results with high precision.

Keywords: Charge distribution; elastic and inelastic scattering; kaon-induced reactions

El estudio de la estructura nuclear para los elementos ^{3}He and ^{4}He ha sido realizada usando cambios de fase para la reacción K$^+$N a intervalos de energía hasta 900 MeV. El análisis y comparación con previos resultados experimentales y teóricos ha sido realizado, obteniendo mejores resultados con alta precisión.

Descriptores: Distribución de la carga, dispersión elástica e inelástica; reacciones del kaon-inducida.

PACS: 21.10.Ft, 25.55.Ci, 25.80.Nv

1. Introduction

The study of the elastic scattering cross section, total cross section and integrated elastic scattering cross section was conducted for the hadronic scattering of K$^+$ from ^{3}He and ^{4}He.

This new analysis wass carried out using previous results from the partial-wave analysis of K$^+$N scattering [1] (GA) in the momentum range from 0 to 1.6 GeV/c. I also compared this with the phase shift analysis from Hyslop *et al.* [2] and Martin's phase shift [3].

The present work focuses on K$^+$ scattering for the isotopes ^{3}He and ^{4}He considering kinetic energies in the range 100-900 MeV.

This complete study was possible thanks to recent K$^+$N phase shifts analysis from Gibbs *et al.* [1] obtained for $I = 0$, 1 with great accuracy.

2. Theory

2.1. K$^+$ -nucleon scattering

The phase-shift analysis for the meson K$^+$ was done using experimental data taken from the Particle Data Group and the experiments carried out at the BNL (Brookhaven National Laboratory).

The partial-wave amplitudes are the results of the following relation:

$$F_{l\pm} = \frac{(S_{l\pm} - 1)e^{2i\sigma_l}}{2i}; \qquad S_{l\pm} = \eta_{l\pm} e^{2i\delta_{l\pm}} \tag{1}$$

in which the sign $\pm$ corresponds to $j = l \pm 1/2$ and σ_l is the Coulomb phase shift.

The differential cross section, total cross section, and integrated elastic cross section are expressed in terms of amplitudes. The derivation of these concepts is given in the Refs. 1 to 4.

2.2. Charge distributions of the helium isotopes and the use of form factors

In this study I have used the charge distribution analyzed by McCarthy *et al.* [5]. The main results are summarized as follows

$$\rho_o(r) = \frac{Z}{8\pi^{\frac{3}{2}}}\left[\frac{1}{a^3}e^{-\frac{r^2}{4a^2}} - \frac{b^2(6c^2 - r^2)}{4c^7}e^{-\frac{r^2}{4c^2}}\right] \tag{2}$$

$$\Delta\rho(r) = \frac{Zpdq_o^2}{2\pi^{\frac{3}{2}}}\left[\frac{\sin(q_o r)}{q_o r} + \frac{p^2}{2q_o^2}\cos(q_o r)\right] e^{-\frac{p^2 r^2}{4}} \tag{3}$$

This fit to the charge distribution for the ^{3}He is

$$\rho(r) = \rho_o(r) + \Delta\rho(r).$$

The best fit values for the parameters of ^{3}He charge distributions are $a = 0.675 \pm 0.008$ fm, $b = 0.366 \pm 0.025$ fm, $c = 0.836 \pm 0.032$ fm, $d = (-6.78 \pm 0.83) \times 10^{-3}$ fm, $p = 0.90 \pm 0.16$ fm^{-1}, $q_o = 3.98 \pm 0.09$ fm^{-1}. The root mean square radius of the last distribution is $r_{rms} = 1.88 \pm 0.05$ fm.

The ^{4}He data were fitted with the two charge distributions used earlier in Ref. [7]. The three parameter Fermi density is

$$\rho(r) = \frac{\rho_o[1 + w(\frac{r^2}{c^2})]}{1 + e^{\frac{(r-c)}{z}}} \tag{4}$$

The best fit parameters for the three parameter Fermi distribution are $w = 0.517 \pm 0.016$ fm, $c = 0.964 \pm 0.012$ fm, and $z = 0.322 \pm 0.007$ fm. The r_{rms} that corresponds to this fitted charge distribution is 1.71 fm.

In the literature there are experiments for the ^{3}He and ^{4}He charge form factor (F_{ch}, F_{mag}) which are described in Refs. 13 to 16 and 18.

In the Born approximation, the two form factors F_{ch} and F_{mag} are identified with the Fourier transform of the spatial distribution of the charge and magnetic moment:

$$F_{ch}(q^2) = \frac{4\pi}{Zq}\int_0^\infty \rho(r)\sin(qr)rdr$$

where

$$F_{ch}(0) = 1,$$

$$\rho(r) = \frac{Z}{2\pi^2}\int_0^\infty \frac{q}{r}\sin(qr)F_{ch}(q^2)dq,$$

and we have a similar expression for the form factor (F_{mag}).

The differential scattering cross section for the spin-(1/2) He^{3,4} is calculated also in the Born approximation with the use of the two form factors (F_{ch}, F_{mag}) and discussed in Refs. 13 and 17.

2.3. Optical Potential

The optical potential is based on a three-body system of kaon (K), nucleon (N), and residual nuclear core (C). This potential was derived in Refs. 8 and 9. The main results are,

$$\begin{aligned}
&\langle \overrightarrow{k}'|V(E)|\overrightarrow{k}\rangle \\
&= \sum_A \sum_{A'} \int d\overrightarrow{q}' d\overrightarrow{q}\, \phi_A^*(\overrightarrow{q}')\widetilde{\phi}_{A'}^*(\overrightarrow{q}' + c\overrightarrow{k}') \\
&\quad \times \langle -a\overrightarrow{q}' + b\overrightarrow{k}'|t_{KN}(E + E_A - \widetilde{E}_{A'})| - a\overrightarrow{q} + b\overrightarrow{k}\rangle \\
&\quad \times \widetilde{\phi}_{A'}(\overrightarrow{q} + c\overrightarrow{k})\phi_A(\overrightarrow{q}) \qquad (5)
\end{aligned}$$

where $\overrightarrow{k}$ and $\overrightarrow{k}'$ are kaon momenta in the kaon-nucleus center of mass frame (3 cm). The matrix $t_{KN}(q)$ is derived in Ref. 10, chapter 13. The quantities a, b, and c are given approximately by,

$$a = \frac{w_K}{w_N + w_K},$$

$$b = \frac{w_N(w_K + w_N + w_C)}{(w_N + w_C)(w_K + w_N)},$$

$$c = \frac{w_C}{w_N + w_C}$$

where all the energies are computed in the 3 c.m.

The main derivation from the optical potential is also presented in Ref. 9 Eq. (6), which after partial wave analysis is reduced to

$$\begin{aligned}
\langle \overrightarrow{k}'|V(E)|\overrightarrow{k}\rangle &= \sum_L [\frac{2L+1}{4\pi}]P_L(cos\theta)\upsilon(bk')\upsilon(bk)\sum_{AA'} b_o(E + E_A - \widetilde{E}_{A'})B^L_{AA'}(k,k') + b_1(E + E_A - \widetilde{E}_{A'}) \\
&\bullet\ [b^2 D^L_{AA'}(k,k') - abE^L_{AA'}(k,k') - abE^L_{AA'}(k',k) + a^2 F^L_{AA'}(k',k)] \qquad (6)
\end{aligned}$$

The term $\upsilon(q)$ and the tensor $E^L_{AA'}$ are given in Ref. 9 [Eqs. (5), (7) and (8)].

3. Results

3.1. Elastic Scattering

Figure 1 presents the elastic scattering for the ^{3}He at different energies in the range 100-900 MeV using the off-shell parameter from $\alpha = 300$, 600 and 900 MeV/c and using the phase shift analysis from Gibbs *et al.* [1].

Figure 2 gives the analysis for the isotope ^{4}He for α=300, 600 and 900 MeV/c in the same range of energies as the K$^+-^3$He nucleus.

Considering the isotope ^{3}He, it is observed that the off-shell parameter $\alpha = 300$ MeV/c has a variation from the parameters $\alpha = 600$ and 900 MeV/c of around 5 to 10% in the elastic differential cross section scattering. Also observing in the Fig. 1 for the off-shell parameter, $\alpha = 600$ and 900 MeV/c, the difference in the elastic scattering is 1 to 2%. Increasing the off-shell parameter, the elastic differential cross section is unaffected.

Doing the same analysis for the isotope ^{4}He, the relative difference is the same for the elastic differential cross section varying the off-shell range parameter as the ^{3}He isotope.

3.2. Total cross section and integrated elastic cross section

In Fig. 3, the total and integrated elastic scattering cross section is analysed using the phase-shift analysis from Gibbs *et al.* [1] for the isotopes (^{3}He,^{4}He). In this figure the total cross section is analyzed considering $\alpha = 900$ MeV/c and the difference for these isotopes is around 30%. The data for the total cross section for ^{4}He come from [12]. The integrated elastic cross section is also shown in this plot for both isotopes, and the difference is around 40 to 50 %.

The real and imaginary parts for the forward amplitude are shown in Fig. 4 as a function of kaon laboratory energy. In this plot I consider an off-shell parameter of $\alpha = 900$ MeV/c. The difference for the isotopes (^{3}He,^{4}He) between these amplitudes, for the real amplitude f(0°) is 15 to 30%, for the imaginary amplitude f(0°) is 25 to 35%.

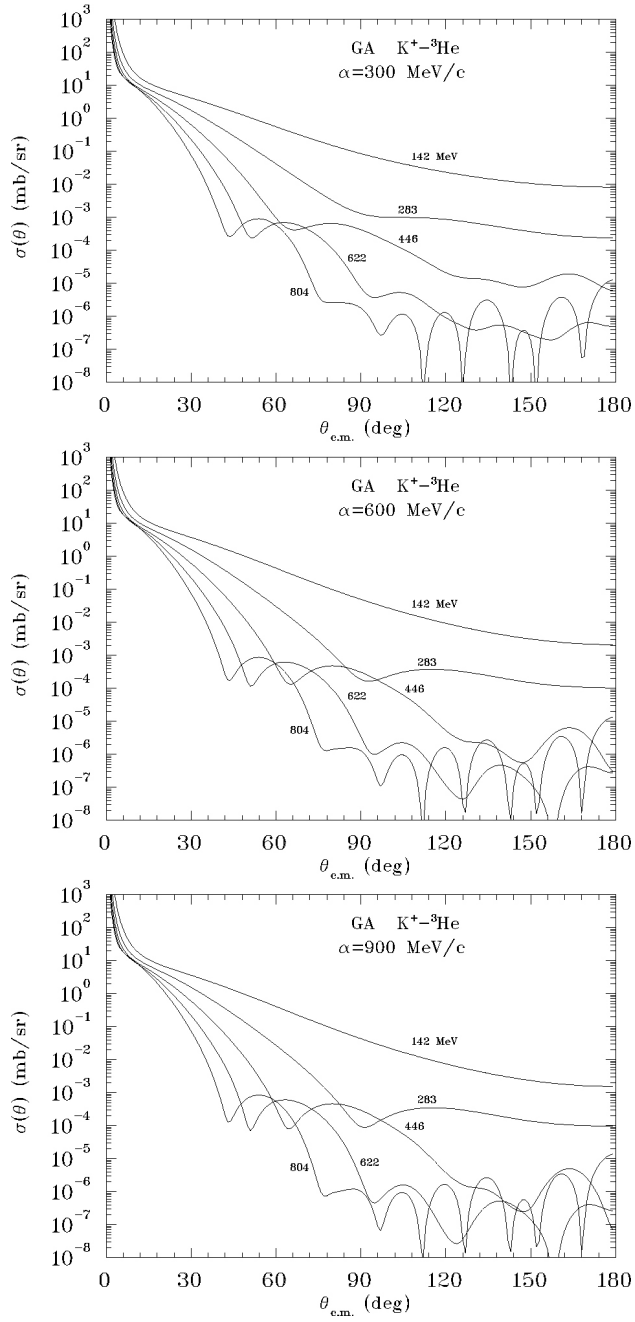

FIGURE 1. K^+ -^{3}He elastic scattering for $T = 142 - 804$ MeV plotted as a function of the angular distribution. It is considered an off-shell parameter from $\alpha = 300$, 600 and 900 MeV/c and using the phase shift analysis from Gibbs *et al.* [1].

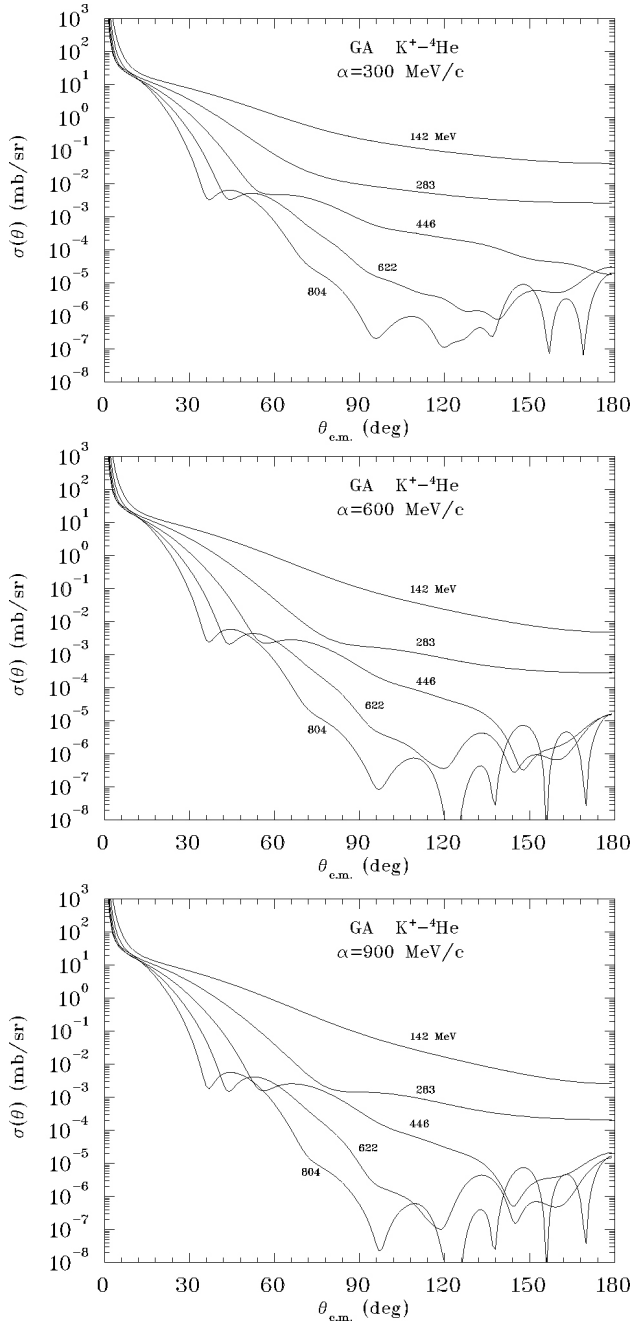

FIGURE 2. K^+ -^{4}He elastic scattering for $T = 142 - 804$ MeV plotted as a function of the angular distribution. It is considered an off-shell parameter from $\alpha = 300$, 600 and 900 MeV/c and using the phase shift analysis from Gibbs *et al.* [1].

3.3. Elastic scattering using the phase shift from Hyslop *et al.* [2], Martin *et al.* [3] and Gibbs *et al.* [1]

Using the phase shift analysis from Hyslop *et al.* [2], Martin *et al.* [3] and the recent results obtained from Gibbs *et al.* [1], for the off-shell parameter α=900 MeV/c, the elastic scattering is compared in order to find some discrepancy in the three different phase shift analyses. This is done because the techniques used to find the phase shifts are different from one group to another. I compare these results with the different values of the kaon internal laboratory energy.

For the isotope ^{3}He, using energies of 283, 446 and 897 MeV, the elastic differential scattering is shown in Fig. 5. In this plot the elastic scattering agrees for the three groups except in some values of the angular distribution. When an energy of 283 MeV is considered, the elastic scattering disagrees between 85-90°. The elastic scattering agrees for Martin's phase shift and Hyslop *et al.*, there is a difference from Gibbs *et al.* around 10%.

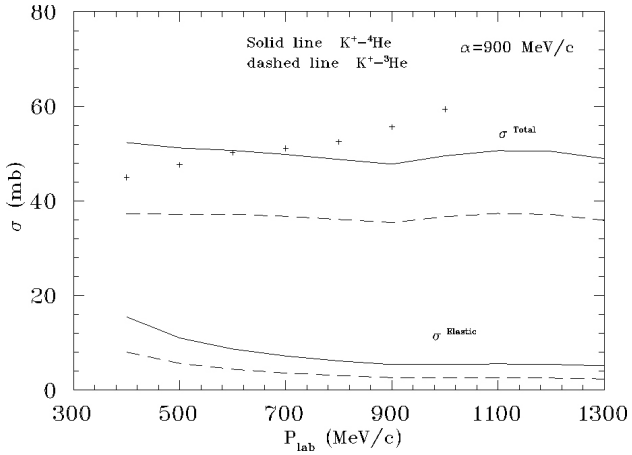

FIGURE 3. The total and integrated elastic scattering cross section for the hadronic scattering of K^+ from (^{3}He,^{4}He) as a function of the laboratory momentum and considering an off-shell parameter of $\alpha = 900$ MeV/c. The points come from [12].

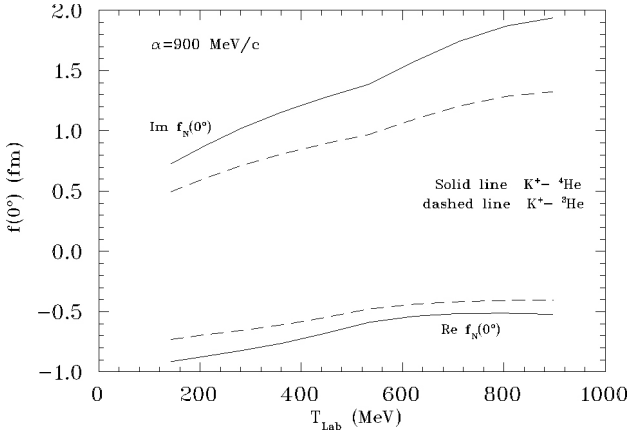

FIGURE 4. The real and imaginary parts of the forward, pure strong amplitude for K^+ scattering from ^{3}He and ^{4}He plotted as a function of kaon laboratory energy and considering an off-shell parameter of $\alpha = 900$ MeV/c.

In Fig. 6 the isotope ^{4}He is considered for the elastic scattering, using energies of 283, 446 and 897 MeV. The elastic scattering does not show change in the first half of the angular distribution, but after 90° the difference between the phase shifts from Gibbs *et al.* and the other two groups is around 1 to 8%.

3.4. Ratio of the total cross section to deuterium

The ratio of the total cross sections from helium to deuterium using the phase shift analysis from Gibbs *et al.* [1], Martin *et al.* [3] and Hyslop *et al.* [2] is shown in Fig. 7 for both isotopes. An off-shell parameter of $\alpha = 900$ MeV/c is considered and it is observed that the off-shell range parameter affects 1 to 5% to the total cross section. Also I observe in this plot that, by making some variation to the off-shell parameter, the ratio will not be affected.

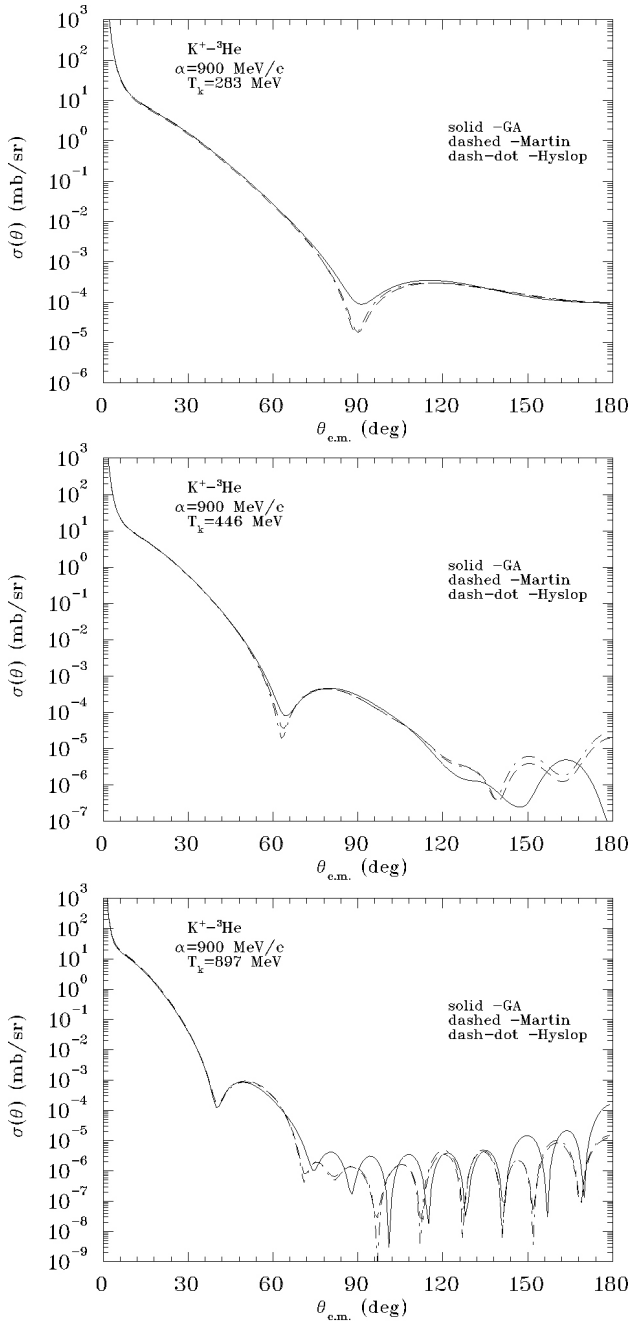

FIGURE 5. K^+ -^{3}He elastic scattering for $T = 283$, 446 and 897 MeV plotted as a function of the angular distribution. Off-shell parameter from $\alpha = 900$ MeV/c is considered, and using the phase shift analysis from Gibbs *et al.* [1], Martin *et al.* [3] and Hyslop *et al.* [2] are used.

3.5. Ratio of the elastic differential cross section from ^{4}He to ^{3}He

The ratio of the elastic differential cross section from ^{4}He to ^{3}He is calculated and shown in Fig. 8. Off-shell parameter of $\alpha = 900$ MeV/c is considered, and a kaon laboratory energy of 446 MeV.

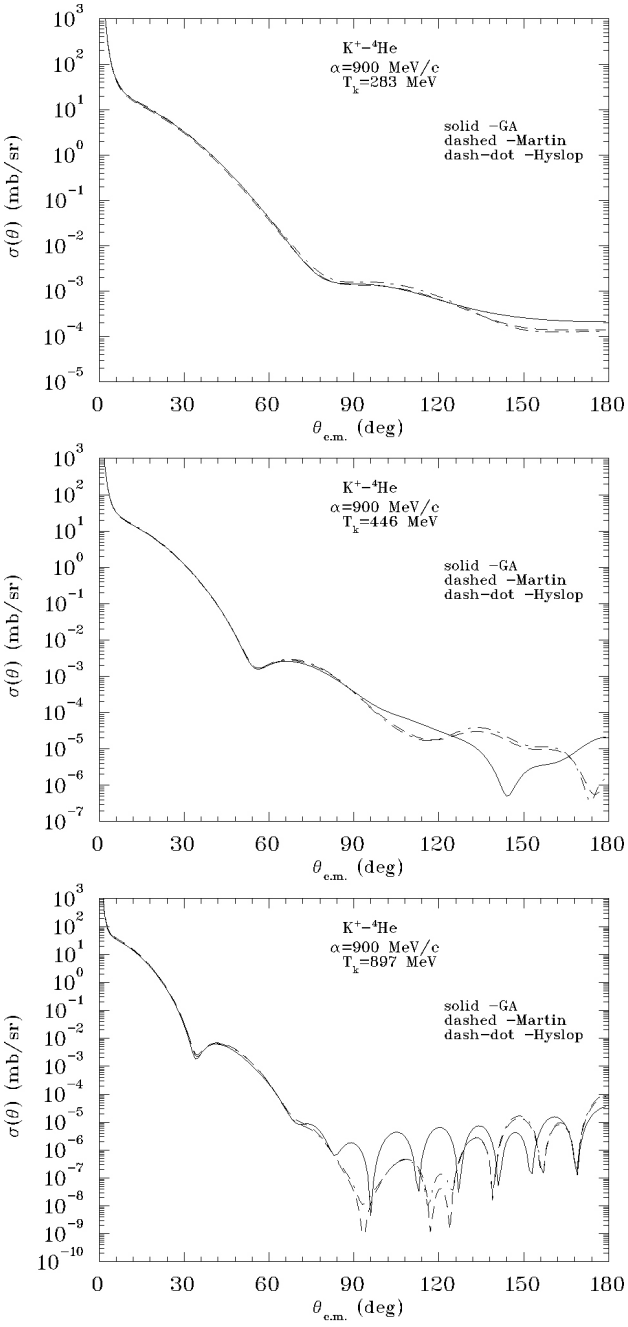

FIGURE 6. The same caption from Fig. 5 but for the reaction K^+ -^{4}He.

The relative difference in K^+ scattering from ^{3}He and ^{4}He at 446 MeV is calculated in Fig. 9. This plot is considering $\alpha = 900$ MeV/c and the recent results from Gibbs *et al.* [1].

$$D(\theta) = \frac{[\sigma(\theta)(^4He) - \sigma(\theta)(^3He)]}{[\sigma(\theta)(^4He) + \sigma(\theta)(^3He)]} \qquad (7)$$

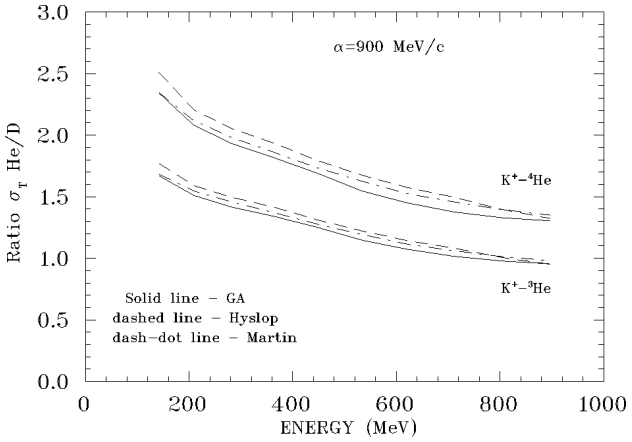

FIGURE 7. Ratio of the total cross sections from helium to deuterium using results from Gibbs *et al.* [1], Martin *et al.* [3] and Hyslop *et al.* [2]. The off-shell range parameter of $\alpha = 900$ MeV/c is considered.

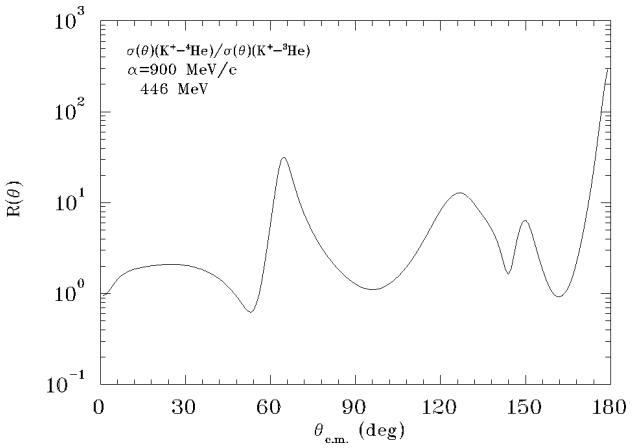

FIGURE 8. Ratio of the differential cross section for K^+ elastic scattering from ^{3}He and ^{4}He at 446 MeV considering $\alpha = 900$ MeV/c.

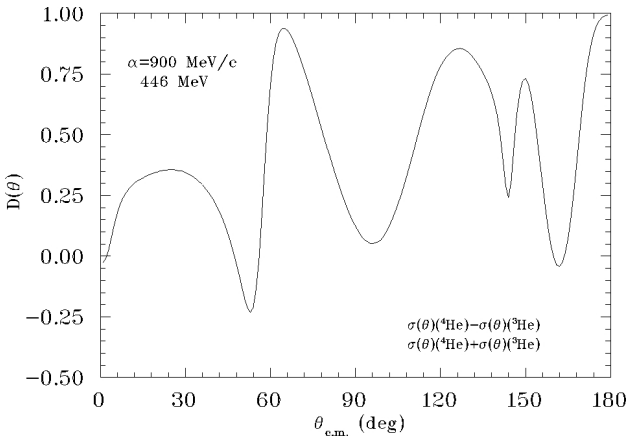

FIGURE 9. The relative difference in K^+ scattering from ^{3}He and ^{4}He at 446 MeV considering $\alpha = 900$ MeV/c.

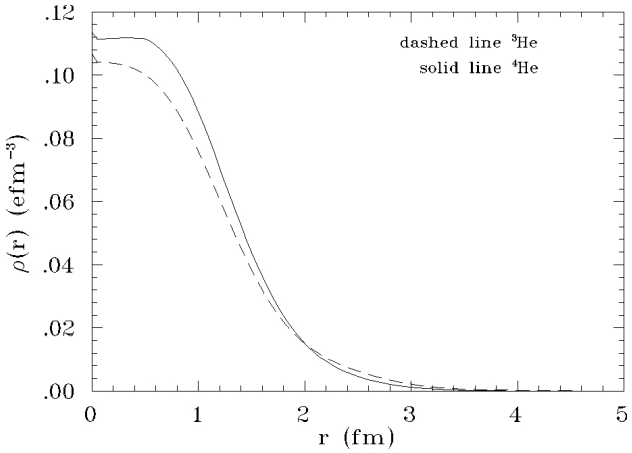

FIGURE 10. Charge distribution for the isotopes ^{4}He and ^{3}He [Eqs. (2)-(4)].

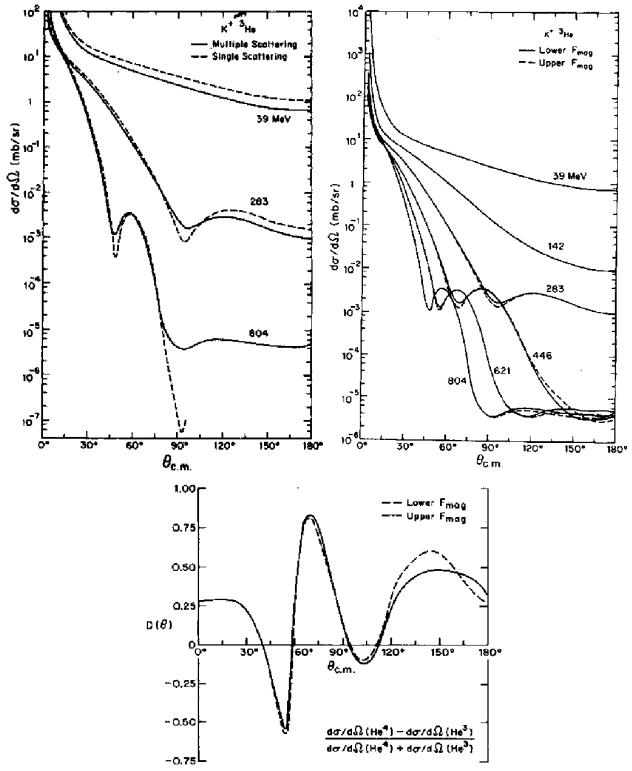

FIGURE 11. K$^+$ -^{3}He elastic scattering as calculated by solving the Lippmann-Schwinger equation and varying the parameters in the input F_{mag}(^{3}He). Also shown is the relative difference Eq. (7).

3.6. Charge electric density for the isotopes ^{3}He and ^{4}He.

The charge electric density is shown in Fig. 10 using Eqs. (2)-(4) and the fit parameter obtained by McCarthy *et al.* [5]. In these charge distributions the best fit parameters are used. The χ^2 per degree of freedom is 0.7, which correspond to the ^{3}He isotope. The χ^2 for the ^{4}He is 0.7. These calculations were obtained by using phase shift analysis.

3.7. Nuclear structure effects in k$^+$ elastic scattering from helium

Figure 11 is taken as in Ref. [11]. In these figures the K$^+$-^{3}He elastic scattering is calculated by solving the Lippmann-Schwinger equation, the same calculation but using a spin distribution obtained by varying the parameters in the input F_{mag}(^{3}He) and the relative difference which is given in Eq. (7). Observing Figs. 1 and 11 , the first figure was calculated using the phase shifts analysis from Gibbs *et al.*, the relative difference around 1-2% between these plots. Also the Figs. 5, 9 agree with Fig. 11.

4. Conclusions

The analysis for the K$^+$ -^{3,4}He nucleus scattering was done. The elastic differential cross section, total cross section and integrated elastic cross section were analyzed with high precision. The use of phase shift analysis from the three different groups and the relative difference between them was found. These results suggest that the use of phase shifts is relevant in obtaining the nuclear structure for both isotopes (^{3}He, ^{4}He).

The ratio of the total cross section from ^{3,4}He to deuterium is calculated and the agreement from the three different phase shift analyses was found (a relative difference around 1-2%). Also the ratio from the elastic scattering from both isotopes was done and the relative difference between them was shown.

The use of a charge distribution was necessary to perform the calculations; the best fit was taken from previous results and shown in some plot.

1. W.R. Gibbs and R. Arceo, *Phys. Rev. C* **75** (2007) 035204.
2. J.S. Hyslop, R.A. Arndt, L.D. Roper, and R.L. Workman, *Phys. Rev. D* **46** (1992) 961.
3. B.R. Martin, *Nucl. Phys. B* **94** (1975) 413.
4. K. Hashimoto, *Phys. Rev. C* **29** (1984) 1377.
5. J.S. McCarthy, I. Sick, and R.R. Whitney, *Phys. Rev. C* **15** (1977) 1396.
6. J.P. Repellin *et al.*, *Phys. Lett.* **16** (1965) 169.
7. R.F. Frosch, J.S. McCarthy, R.E. Rand, and M.R. Yearian, *Phys. Rev.* **160** (1967) 874.
8. H. Garcilazo and W.R. Gibbs, *Nucl. Phys. A* **356** (1981) 284.

9. P.B. Siegel, W.B. Kaufmann, and W.R. Gibbs, *Phys. Rev. C* **30** (1984) 1256.
10. W.R. Gibbs, "Computation in Modern Physics", *World Scientific Publishing*, (Third Edition 2006).
11. M.J. Paez and R.H. Landau, *Phys. Rev. C* **24** (1981) 1120.
12. R. Sawafta *et al*., *Phys. Lett. B* **307** (1993) 293.
13. J.S. McCarthy, I. Sick, R.R. Whitney, and M.R. Yearian, *Phys. Rev. Lett.* **25** (1970) 884.
14. M. McMillan, *Phys. Rev. C* **3** (1971) 1702.
15. R.H. Landau, *Phys. Rev. C* **15** (1977) 2127.
16. B.F. Gibson and L.I. Schiff, *Phys. Rev.* **138** (1965) B26.
17. H. Collard, R. Hofstadter, E.B. Hughes, A. Johansson, and M.R. Yearian, *Phys. Rev.* **138** (1965) B57.
18. L.I. Schiff, *Phys. Rev.* **133** (1964) B802.